Removal of phenol from aqueous solution using biochar produced from Araucaria Columnaris Bark

Dinesh Chandola*[1], Pooja Thathola[1] and Ankit Bisht[2]

Email: *chandola.dinesh@gmail.com, poojathathola29@gmail.com* and *abisht135@gmail.com*

[1]G B Pant National Institute of Himalayan Environment (GBPNIHE), Kosi-Katarmal, Almora - 263643, India

[2]IMS Unison University (IUU), Dehradun -248001, Uttarakhand, India

*Corresponding Author email: Dinesh Chandola, *Chandola.dinesh@gmail.com*

Abstract

This work investigates the removal of phenol from aqueous solution using Araucaria Columnaris bark (ACB) as biochar. Five different types of biochars were developed through pyrolysis at different temp from 300 to 500°C. The effects of initial concentration, contact time, pH and temperature on adsorption behavior were studied in batch mode for each biochar. The optimum contact time observed for equilibrium condition was 60 mins for every biochar. And, the maximum adsorption followed the order 298 K > 308 K > 318 K. Adsorption equilibrium data were fitted to Langmuir and Freundlich isotherms by non-linear regression method and kinetic data by linear regression method, and fitted to pseudo-first order, pseudo-second order and Intraparticle diffusion models. Adsorption kinetics was reasonably described by pseudo-second order model with R^2 value 0.99. Thermodynamic parameters were also estimated that implied, the adsorption process was spontaneous and exothermic in nature. Study further showed that the acidic pH increased adsorption capacity of biochar but decreases continuously towards basic side. The removal of phenol with prepared biochar was achieved as high as 100 % for ACB-500. The maximum iodine adsorption value of prepared biochar was found to be 453.3 mg/g.

Keywords: *Biochar preparation and characterization, reaction kinetics and isotherm study, Phenol removal and thermodynamic study.*

1. Introduction

Phenols are widely used for the commercial production of a wide variety of resins including epoxy resins, adhesives, phenolic resins that are used as construction materials for automobiles and polyamide for various applications [1]. These are becoming common sources for phenolic contaminants in wastewaters [2]. Phenols as a class of organics are similar in structure to the more common herbicides and insecticides which are resistant to biodegradation [3]. It is therefore, recommended to remove the phenol from waste water effluents before entering into the water stream [4]. The united State Environment and Protection Agency (USEPA) and European Union (EU) have already enlisted phenolic compounds as priority concern due to its toxicity and carcinogenic properties. They are very harmful to organisms even at low concentrations which can damage the red blood cells and the liver [5]. The presence of phenolic compounds in the aquatic environment may be from both natural and anthropogenic source. The physical structure of phenol has been shown in Fig.1. Consequently, there are numbers of treatment techniques developed and proposed for the removal of phenol from waste water effluents. Some common techniques include extraction [3], polymerization, electro-Fenton process [6], photo catalytic degradation [7], and adsorption and so on [3]. There are more than thousand different studies reported on adsorption of phenolic compounds on different adsorbents. Amongst them activated carbons has been studied extensively[8][9][10][11]. Biochar for the removal of organic waste are currently produced from a variety of starting materials such as nutshells [9], wastes agricultural residues [12], date pits, wood [13], plum kernels [14] , and polymers [15]. However, its high initial cost and the need for a costly regeneration system make it less economically viable as an adsorbent [16]. Taking these work results as criteria into

consideration, a low cost and easily available Araucaria Columnaris bark based biochar has been investigated for the removal of phenol from aqueous solution.

1.1.Araucaria Columnaris bark as a low-cost material

This plant is also known as Cook pine, because it is a tree native to the Cook Island, north-east of Australia in the South Pacific [17]. It is an ever-green tree and, in India it is a common ornamental plant and often called as 'Christmas Tree'. The height of Cook pine can reach 60 m in natural tendency, and commonly grown as a house-plant in garden and pots. This tree is present almost in every island, commonly known as "Norfolk-Island-pine" in Hawaii. Fig. 2 shows the bark of the tree. The Araucaria Columnaris is an evergreen tree, so there was no special time to extract bark from this tree.

2. Materials and Methods

*2.1.*Chemicals used

Phenol crystalline extra pure (assay ≥ 99.9%) with analytical grade from Sisco Research Laboratories was used as an adsorbate. It was dissolved in estimated quantities to prepare stock solutions. De-ionized water, obtained from a Deionizer (Mars Bioanalytical, Zartifikal) has been used through the experiment. During batch adsorption studies, the pH was maintained with 0.1 M HNO_3 and 0.1 NaOH solutions. For desorption experiment, NaCl (assay ≥ 99.9%) was purchased from Sisco Research Laboratories Pvt. Ltd. and NaOH (assay≥ 98%) from Himedia Laboratories Pvt. Ltd.

2.2. Methods

In this study, the materials were first developed and characterized by different analytical methods. After that, their adsorption properties were examined in batch mode. The experimental

procedures were prepared after referring several studies in this field during recent years. Details of the methods are given below.

2.2.1. Preparation of biochar

The raw material for biochar production was the bark of Araucaria Columnaris tree. The bark samples (of light brown color) were collected during January from the lower Himalaya region of north India. After collection, the bark was thoroughly washed with tap water to remove the dust, soil, and any other foreign substances. The washed samples were then spread on newspapers and allowed to dry in sunlight for next 5 days. After five days, the samples were further dehydrated in oven at 60 °C for 24 hours. Thereafter, sample was crushed into rust colored powder with help of an electric grinder. The powder was sieved through 0.5 mm mess size. Further, this powder was pyrolyzed at five different temperatures i.e. 300, 350, 400, 450 and 500 °C.

2.2.2. Pyrolysis of biochar

Slow pyrolysis was performed to produce the biochar; 150 g powder sample of Araucaria Columnaris bark was weighed in Aluminum-foil made boat and heated in a muffle furnace model no. NSW 103 (Narang Scientific Works) according to different heating program, given in Fig.3. The reaction mechanisms for biomass pyrolysis are complex but can be understood in three main steps [18]:

$$Biomass = water + unreacted\ residue \quad (1)$$

$$Unreacted\ residue = (Volatile + Gases)_a + Char_a \quad (2)$$

$$Char_a = (Volatile + Gases)_b + Char_b \quad (3)$$

When biomass is pyrolyzed in muffle furnace, initially moisture and volatile fraction is lost and, unreacted residue left (Eq. (1)). Later, in the second step, biochar formation takes place (Eq. (2)).

And, in the final step some chemical rearrangement also occurs at a very slow rate and carbon-rich residual solid forms along with the formation of secondary charring (Eq. (3)). In this study, pyrolysis temperature was set to increase at 10°C/min with continuous supply of nitrogen gas at a rate of 750 ml/min. The maximum temperature was set at 500°C .The furnace was then retained at a specific duration (one hour) before the furnace was shut off. Even during cooling, nitrogen supply was maintained to prevent the oxygen exposure to the char. A set of five treatment temperature for biochar production e.g. 300, 350, 400,450 and 500 °C was selected. Once the furnace cooled down to room temperature, the sample were collected and weighed for calculation of weight loss during pyrolysis. The black colored samples so obtained were homogenized by crushing and mixing the lumps developed during pyrolysis. The samples were stored in desiccators before further use and labeled as ACB-300 (Araucaria Columnaris biochar developed at 300°C), ACB-350 (Araucaria Columnaris biochar developed at 350°C), ACB-400 (Araucaria Columnaris biochar developed at 400°C), ACB-450 (Araucaria Columnaris biochar developed at 450°C) and ACB-500 (Araucaria Columnaris biochar developed at 500°C).

2.3. Biochar characterization

2.3.1. Biochar yield

The biochar yield (ɳ) has been expressed in weight percentages (wt. %) of dry ash-free biochar recovered to dry ash-free initial biomass. Dry ash-free basis for yield expression was chosen to avoid positive bias in yield in case of using biomass samples with high mineral (ash) content. The yields (ɳ) were calculated by (Eq. (4))

$$ɳ=(V_C - V_{ash,\,c})/(V_{dry,\,b} - V_{ash,\,b}) \times 100 \quad (4)$$

Where V_C is the wt. of the char recovered during the pyrolysis process in g, $V_{dry, b}$ is the oven-dry mass of raw biomass material and $V_{ash, c}$ and $V_{ash, b}$ represent the respective ash contents in the biochar and raw biomass samples (wt. in g).

2.3.2. Proximate analysis

Volatile matter, moisture and ash content were estimated according to D1762-84 (ASTM, 2007). Briefly, 1g biochar samples were heated in porcelain crucibles and the difference in the sample weight after and before heating were calculated. To estimate the moisture content, samples were dried for 2hrs at 105°C in dry oven. Similarly, for volatile matter, the samples were heated for 11min at 950 °C in covered crucible and for ash content sample were heated at 750 °C for a minimum of 2 hrs in uncovered crucible. Subtracting the weight of the moisture content, ash content and volatile matter content from original sample gives the value of stable carbon fraction of that sample. Hence, this fraction is termed 'fixed carbon or fixed-C fraction'. In this study, the fixed carbon fraction is expressed on dry ash-free basis given by (Eq. (5))

$$\%f_c = 100\ (V_{dry} - V_{vm} - V_{ash})/(V_{dry} - V_{ash}) \quad (5)$$

Where % f_c is the fraction of fixed carbon (in wt. %), V_{vm} is the weight of volatile matter in the sample (g), V_{dry} is the oven dry weight of the sample (g) and V_{ash} is the weight of the ash residue of the sample (g). In this study, ratio (in wt. %) of weight of fixed carbon in a biomass sample to the weight of the original biomass feedstock on a dry and ash-free basis is defined as the fixed carbon yield expressed by (Eq. (6))

$$\%Y_{fc} = \%f_c\ (V_{dry,\,c} - V_{ash,\,c})/(V_{dry,\,b} - V_{ash,\,b}) \quad (6)$$

Where $\%Y_{fc}$ is the fixed carbon yield (in wt. %), $V_{dry,\,c}$ and $V_{dry,\,b}$ are the dry weights (g) of the biochar and the biomass feedstock respectively. And, $V_{ash,\,c}$ and $V_{ash,\,b}$ are the weights (g) of the ash in the biochar, and in the original biomass feedstock, respectively.

2.3.3. Elemental analysis

The elemental analysis (CHNS) was done using a Flash-2000 Elemental Analyser (Eltra). The biochar samples were weighed and wrapped in tin boats as per the standard procedure. The daily factor was determined with sulphanilamide and the samples are analyzed subsequently.

2.3.4. Surfaces characteristics

In this study, For quantification of the surface functional groups, Boehm's titration was done by using the method described by [19]. Briefly, 1g biochar sample was added to 50 mL solution of different bases (0.01N $NaHCO_3$, Na_2CO_3 and NaOH respectively). The mixture was shaken in room temperature for 48 hrs. The biochar samples were separated by filtration. The quantities of functional group were determined by back titration with 0.05 N standard HCl solutions. Same amount of solution without carbon were used as blank. The total surface basicity of the biochar samples were quantified by mixing 1.0 g of the carbon sample with 50mL of 0.05N standard solution of HCl. The suspension was shaken for 24 h at 25°C. An aliquot of the supernatant was filtered and back titrated with 0.05N solution of NaOH.

2.3.5. Biochar surface area estimation by Iodine Number

The adsorption of aqueous iodine is considered a quick test for evaluating the surface area of biochar. It was determined according to the procedure established by the American Society for Testing and Materials (ASTM). The powered biochar is grinded until 60 wt. % to 95 wt. % or more is passed through a 100 mesh screen. Further, a mass of 0.1 g of the biochar was placed in

100 mL conical flask and 5 mL of 5% HCl added to it. The flask was swirled until the biochar was wetted and 10 mL 0.1 M iodine solution was added. Then 10 mL of the filtrate was titrated against a standard 0.1 M sodium thiosulphate solution. The concentration of iodine adsorbed is equivalent to the surface area of the activated carbon.

2.3.6. pH in solution

Biochar samples were suspended in a 0.1 N KCl solution in a 1: 10 (wt. /wt.) ratio. After 10 min of stirring, the pH of the biochar suspension was measured using a Model 420 Thermo-Orion (Thermo Fisher Scientific). The analyses of pH were performed in duplicate.

2.3.7. Determination of pH_{zpc}

To determine of pH value of the prepared biochar at the point of zero charge, 50 mL NaCl solution of 0.1 M was taken into 100 ml glass tubes. The initial pH was maintained between 2 and 11 by adding 0.1 M HCl or 0.1 M NaOH. Once the pH was maintained, 0.5 g prepared biochar was added to the solutions and the glass tubes were put into rotatory shaker with a speed of 150 rpm at 25°C. After 24 hrs, the suspensions were filtered by cellulose acetate membrane filters of pore size 0.45μ and final pH of the filtrates was measured. The difference between the initial and final pH values ($pH = pH_i - pH_f$) was plotted versus pH_i. The pH at which pH = 0 is as pH value at the point of zero charge [20].

1. **Batch mode study**

The batch-scale experiments were carried out to evaluate the adsorption behavior of prepared biochars on phenol removal, under different experimental conditions. In these experiments, effect of contact time, effect of initial concentration, temperature and pH were investigated. Two

isotherm models Langmuir and Freundlich were used along with three kinetic models e.g. pseudo first, pseudo second, and Intraparticle diffusion. To evaluate the final concentration of phenol, spectrophotometer (Labtronics) was used at wavelength 270 nm. The amount of adsorbate adsorbed on the adsorbent is calculated by using mass- balance (Eq. (7)):

$$q_e = (C_0 - C_e)/W \times V \quad (7)$$

Where, q_e is the final amount of phenol adsorbed on adsorbent (mg/g), C_o is the initial concentration of phenol at time ***t.*** C_e is equilibrium concentration (mg/L) of phenol at equilibrium state. And, *W* is the weight of the adsorbent and V is the volume of solution in L.

1.1. Study of Contact Time

This experiment was carried out to evaluate the equilibrium time for phenol adsorption. A stock Solution of 500 mg/L was prepared by dissolving 500 mg of phenol powder in 1 liter Millipore water. The working solution of 100 mg/L in 210 mL was prepared and to this 0.5 gm. of adsorbent was added. Before adding the adsorbent in solution, the initial sample concentration was determined using spectrophotometer. The solutions was placed on stirrer for next 3 hrs meanwhile at regular interval of time 1, 2, 3, 4, 5, 10, 15, 20, 30, 40, 60, 120, 180 min the sample were withdrawn. The final solution was filtered through syringe filter and filtered solution was analyzed using spectrophotometer.

1.2. Effect of pH on adsorption

The effect of pH on adsorption in term of its removal efficiencies was observed. Solution of 10 different sets of 100 mg/L in 50 mL were prepared from 500 mg/L of stock solution and then maintained at pH of 2, 3, 4, 5, 6, 7, 8, 9, 10, 11, 12 using acid (0.1 M HNO_3) and base (0.1 M NaOH) solution respectively. After maintaining the pH, 0.5 gm. of materials was added in all the

Erlenmeyer flask and was placed on stirrer cum water bath for 2 hrs under continuous stirring. The initial and final concentrations of all 10 solutions at different pH were calculated.

1.3. Effect of initial concentration

This experiment was performed to determine the effect of initial concentration of phenol on adsorption capacity of biochar. A total of 10 (10, 20, 30, 40, 50, 60, 70, 80, 90, 100, mg/L) working concentrations were prepared from 500 mg/L phenol solution. The amount of 50 mL of each concentration was taken into Erlenmeyer flasks and 0.5 g adsorbent was added to each set-up and allowed to stir for 2 hrs at temperature 298 K.

*1.4.*Effect of temperature

Temperature plays a very crucial role in adsorption process. Therefore, the effect of temperature on adsorption capacity was observed. In this experiment the variation in adsorption capacity were observed in three different temperatures (298, 308, and 318 K). For this experiment 50 mL working solutions of 10, 20, 30, 40, 50, 60, 70, 80, 90, 100 mg/L in an Erlenmeyer flask were prepared from stock solution (500 mg/L). All working solution was divided in two sets of initial and final parts of each having 5 mL and 45 mL of solution. Initial were in vials and final solution were in Erlenmeyer flasks to which 0.5 gm. of adsorbent were added and kept for 2 hrs of continuous stirring on stirrer cum water bath at desired temperature.

*1.5.*Desorption

Desorption study was done by filtering the phenol solution and gently washing the filter paper with milli-Q water so as to removal the biochar adsorbed with phenol. The biochar was mixed with three desorbing agent namely; deionized water, NaCl and NaOH. These solutions were

stirred till equilibrium time. Desorbed phenol was then analyzed by spectrophotometer. And, the biochar was again tested for reusability by the method prescribed above. The change in adsorption and desorption amount after each cycles was calculated in terms of %, where, initial adsorption amount was taken as 100 %.

2. Results and discussion

2.1. Characterization

2.1.1. Biochar yield

The effects of temperature and pyrolysis residence time on biochar yield are illustrated in Fig. 4. When the pyrolysis temperature increased from 300°C to 400°C, the biochar yield sharply decreased from 72.2 wt. % to 30.0 wt. %. This was possibly due to most of the Lignocellulosic material was decomposed at this temperature range and more volatile matter were released [21]. While, the pyrolysis temperature further increased from 450 to 500 ◦C, the biochar yield decreased only from 37.4 wt. % to 30.0 wt. %. This indicated that most of the volatile fraction had been removed at lower temperature which is also clear from the table 1, only 8.14 wt. % of volatile matter left at 500 °C. Almost 62.3 wt. % of volatile matter volatilized at temp 350 °C. Also, at higher temperature 500 °C, the sample had a high ash content (13.55 wt. %) which may act catalytically during the pyrolysis process and alter the product distribution in terms of yield of gas and char [22]. Also, higher temperature largely alters the biochar's internal structure and surface [23]. Fixed carbon yield was highest at 500 °C which is free from moisture, volatile fraction and ash content.

2.1.2. Proximate analysis

The volatile matter and fixed carbon for the prepared biochars ranged from 49.4 wt. % to 8.14 wt. % and 22.54 wt. % to 68.44 wt. %, respectively. As the pyrolysis temperature increases the volatile material decreases similar like biochar yield while opposite pattern is seen with the content of fixed carbon. This may be attributed to the increasing temperature further cracks the volatiles fractions into low molecular weight liquids and gases instead of biochar [23]. Along with this, thermal degradation and dehydration of hydroxyl groups of cellulose and lignin might have occurred within the structure of biomass with the increasing temperature [24]. These results further confirms that the increase in temperature enhanced the stability of biochar for the loss of volatile fractions [25]. It was also observed that the ash content increased from 3.4 wt. % to 12.05 wt. % with an increase in the pyrolysis temperature from 300°C to 450°C. The increase in the ash content may be due to the concentration of inorganic matter and nutrients [26]. At temperature above 450°C to 500°C, some inorganic content and nutrients might have been volatized as gas or liquid resulting in a slight increase in ash content from 12.05 wt. % to 13.55 wt. %.

2.1.3. Elemental Analysis

Table 2 shows the elemental composition of biochar in percent (%). The carbon (C) content increased from 43.11 % to 79.7 %, whereas the sulfur (S) and hydrogen (H) contents decreased from 15.09 % to 2.005% and 7.517 % to 2.22 % as the rise in the pyrolysis temperature from 300 to 500 °C respectively. These results also agrees to the results previously reported by [27]. The decreased contents of H and S at higher temperature were likely due to the desulfurization of sulfur into SO_2, some fraction of sulfur might have retained in fly gas [28]. Along with this, breakdown of the oxygenated bonds might have taken place along with the release of low molecular weight byproducts containing H and S [29]. Surprisingly, the highest N content was

observed in ACB-450 (1.95%). This may be described by the supply of nitrogen gas into the complex structures which were resistant to lower temperature, and at higher temperature it was easily volatilized [27].

2.1.4. Surface characteristics of biochar by Boehm Titration method

The quantities of the acidic and basic groups are presented in Table 3. Boehm titration data indicated that biochars had considerable amount of acidic surface groups at lower temperature and at higher temperature, the increased basic surface groups were observed which was also confirmed by pH_{PZC} (Between 4.7 to 8.47) value. Biochars may carry O-containing and N-containing functional groups on the surface. The O-containing functional groups are divided into acidic functional groups, such as carboxylic, lactonic, and phenolic groups and basic groups, such as quinonoid carbonyl, pyrone and benzopyranyl groups [30] [31]. The high basic functional groups at higher temperature was due to the ash fraction and pH [29]. Hence, highest ash content was observed in ACB-500 (13.55 wt. %) therefore, contained highest total basic groups (1.87 mmol/g). The similar trends has been observed previously by [32][33]. Subsequently, other groups like lactonic and carboxylic groups were decreased to 1.01 mmol/g and 0.38 mmol/g respectively.

2.1.5. pH of biochar

In this study, the pH value increased with increase in pyrolysis temperature as shown in table 1. The pH of ACB-500 was higher than ACB-300. This may be due to the separation of alkali salts from the organic matter [34] and by the formation of carbonates such as $MgCO_3$ and $CaCO_3$ and also, due to the presence of inorganic alkalis such as Na, Ca, K and Mg [27]. But at lower temperature around 180-280 °C, the hemicelluloses and cellulose generally decompose that

produce organic acids and phenolic substances as a result of acidic functional groups such as -COOH and -OH lowers the pH of the biochar [35].

2.1.6. The study of pH_{pzc}

pH_{pzc} signifies the pH at which overall surface charge of the adsorbent becomes zero. And the cation and anion exchange capacity also become equal on adsorbent's surface [36]. Results of this study Fig. 5 shows that the pH_{pzc} of biochar is from 5 to 8.4. When pH of the solution is lower than the pH_{zpc}, net surface charge of biochar is positive due to the adsorption of excess H^+. In this situation, biochar has high ability for the adsorption of anionic species. Also, when pH of the solution is higher than the pH_{zpc}, the net surface charge on surface biochar is negative due to desorption of H^+. In this situation, surface of biochar becomes suitable for desorption of cations.

2.1.7. Effect of pyrolysis temperature on iodine value and carbon yield

As can be seen in Fig. 4, with the increase of temperature (300°C to 500°C), biochar yield decreased from 74.2 to 30.0 % where iodine values increased from 198.8 mg/g to 453.3 mg/g but after 450°C the iodine value decreased . This might be due to the increase in temperature would have enhanced the degree of carbonization subsequently the number of microspores would have increased that led to the increased iodine value [37]. Iodine value initially increased until the pyrolysis temperature reached to 450°C this may be due to the change of pore structure in biochar and however, the pore structure would not increase beyond a certain pyrolysis process [38]. This may be the reason of decreased iodine value at 500°C. In this study, the iodine value and biochar yield were observed at 1hr pyrolysis time.

3. Batch adsorption studies

*3.1.*Effect of initial concentration

To evaluate the uptake capacity of biochar, the initial phenol concentration was varied between 0 to 150 mg/L. Fig. 6, illustrates that adsorption increases as the concentration of phenol increases. The experiment was conducted at pH 7.0; temperature 25 ± 2°C and in water bath at stirring speed of 200 rpm. Increase in the amount of adsorption with increase in its initial concentration is due to the increase in the mass gradient pressure between adsorbate and adsorbent which drives the transfer of the phenol molecule from bulk solution to the surface of biochar.

*3.2.*Effect of pH on adsorption of phenol

The pH was varied from 2 to 12 with 0.1N NaOH and 0.1N HNO_3 solutions. The results from Fig. 7 show that the variation of pH does influence the extent of phenol ionization in the solution and surface charge of adsorbents hence controls the adsorption processes. It is clear from the Fig. 7 that at higher pH; the adsorption of phenol is lower. The reason could be the electrostatic repulsions between the negative surface charge and the phenolate–phenolate anions in solution which has also been explained by [39][40]. At acidic pH, phenol was undissociated and the dispersion interaction dominated. Therefore, from pH 4 to 6 there is slight increase in adsorption followed by decrease from 6 to 7 onwards. It may also be understood by the groups like –OH and –COOH on biochar that usually control the adsorption on its surface. Collectively, these groups in aqueous solution makes surface more negative and in other words more suitable for positive charged species. In present case phenol is a molecule with acidic properties, due to C_6H_5-O—H, which can release H^+ in solution. The pKa of phenol at room temperature is about 9.0 which mean the above pH 9 the phenol remains ionized form, and hence more water soluble, and also less adsorbed. At lower pH the surface of carbon is protonated and reduces the possibility of interaction of phenol with surface, and resulted as lower adsorption.

*3.3.*Effect of contact time on adsorption capacity and reaction kinetics

Once the liquid and solid phase comes in contact, a condition of equilibrium is reached. The time period required to achieve this state under given set of conditions, is called as optimum contact time. The contact time (1 to 360 min) on adsorption of phenol by different biochar was investigated and results are shown in Fig. 8. Figures show that q_e of phenol increased rapidly with increasing contact time up to 60 min for each biochar. The adsorption remained almost constant after this time. Therefore, this time was considered as optimum contact time and in all the subsequent batch experiments, the contact time of 60 mins was fixed to study the influence of other experimental conditions. The adsorption was almost equalized thereafter possibly due to the saturation of surface active sites. However, with increasing pyrolysis temperature, the removal rate and adsorption capacity both increased significantly, the removal rate reached upto 100 % for the biochar prepared at 500℃. When the pyrolysis temperature decreased below 500℃, the removal rate also decreased upto 63.3 % for biochar developed at 300°C. The difference in the adsorption capacity may be attributed to the difference in pore size and pore volume of biochars [32].

Fig. 9A, Fig. 9B and Fig. 9C shows Pseudo-first-order [41], pseudo second-order [42] and the intra-particle diffusion model [43] have been used to investigate the mechanism of adsorption of phenol on biochar. The first-order mechanism can be expressed by the following equation (Eq. (8)):

$$\ln(q_e - q_t) = \ln q_e - k_1 t \quad (8)$$

Where q_e and q_t are the amounts of phenol adsorbed (mg/L) at equilibrium and at time t (min), respectively, and k_1 (min^{-1}) is the rate constant adsorption. Values of k_1 at 25°C were calculated from the plots of ln ($q_e - q_t$) versus t.

The pseudo-second-order model can be expressed by the following equation (Eq. (9)):

$$t/q_t = 1/k_2 qe^2 + t/q_e \quad (9)$$

Where K_2 (mg/g/min) is the rate constant of second order adsorption calculated from the linear plot of t/q_t versus t at 25°C.

Intra-particle diffusion model was also used to analyze and describe the diffusion mechanism using the following equation ((Eq. (10)) :

$$q_t = k_p t\text{^}(1/2) + C \quad (10)$$

Where q_t (mg/L) is the amount of phenol adsorbed at equilibrium at time t, C is the intercept and K_P (mg/g/min) is the intra-particle diffusion rate constant. Values of K_P and C can be calculated from the plot of q_t against $t^{1/2.}$

Comparing the correlation coefficients, R^2 from the three kinetic models (Table 4), biochars reasonably fitted all models, so it was difficult to confirm which adsorption kinetics could be more satisfactorily applied. The obtained R^2 values for the pseudo-second-order model were greater than that for all three models, which suggests the better fit for pseudo-second-order model. But for better understanding, intra-particle diffusion model proposed by Weber and Morris (1993) is able to recognize the diffusion mechanisms and rate controlling steps in the adsorption process. If the adsorption process follows the intra-particle diffusion model, then q_t

versus $t^{1/2}$ will be linear and passes through the origin. However, if the data shows two or more distinct linear plots, then it is believed that adsorption is also controlled by two or more steps. In such a case, the first linear plot represents an external resistance to mass transfer by the surrounding particles. And, the second line plot is the rate-controlling steps involving gradual adsorption either by Intraparticle diffusion or any other mechanism. Fig.9C shows the variation of the amount of phenol adsorbed along with $t^{0.5}$. The figure shows the points are connected to two linear plots. As per the model, the first linear plot represents macropore and mesopores diffusion, whereas the second linear plot characterizes the micropore diffusion of adsorbed species [44]. From all the biochar, ACB-300 shows deviation of the linear plot that passes through the origin, which is possibly due to the difference in the rate of mass transfer in the initial and final stages of adsorption. These deviations also suggest that the pore diffusion is not the only rate-controlling step. It is important to note here, that the initial part of q_t versus $t^{1/2}$ is showing a curvature for all the four biochar, which indicates boundary layer diffusion effect or external mass transfer effects existed.

*3.4.*Adsorption mechanism

The removal of phenol from aqueous solution has been explained by three mechanisms; first hydrogen bond formation; second, π-π interaction and third, electron-donor-acceptor complex formation. Firstly, hydrogen bond formation has been explained by [45] in which, the oxygenated functional groups can prevent shifting of π-electrons of adsorbent surface or/and diminishes π-π interaction between adsorbent surface and phenol molecule which further facilitate H-bond formation with phenol molecules that probably lowers the adsorption process. Second, π-π interaction takes place between π electrons on phenol ring and the π-electron present on the surface of adsorbent [46]. A study by [47] has assumed the surface function

groups (carbonyl, lactone, carboxy and phenol) acts as electron withdrawing groups which results in reduction of π-electron density on biochar surface, hence reduces the adsorption performance of phenol or other aromatic compounds. Third , the electron donor-acceptor complex formation was proposed and explained by [48], the carbonyl group present on the surface of biochar facilitates electron and acts as electron donor and phenol receives the electron and acts as acceptor. However, the oxidation of carbonyl group into carboxyl group does not favour the complex formation hence reduces the adsorption performances. but, research by [49][50] have shown that carbonyl groups may perform as electron donors and phenol as receptors, leading to enhanced phenol adsorption. As per the first and second mechanisms, oxygen containing groups has been found unfavorable to phenol adsorption by carbonaceous material. However, according to the third mechanisms, adsorption may be enhanced by carbonyl groups. Correlating these observations with present study by biochar (Table 3), the ACB-300 has shown highest phenol adsorption capacity (41.9 mg/g) despite having lowest iodine adsorption value (198.8 mg/g); indicating lowest pore and micropore volumes but increased number of` oxygenated groups (3.41 mmol/g of carbonyl functional groups). The ACB-500 attained phenol adsorption capacity 29.96 mg/g and had highest iodine adsorption value (453.3mg/g) but lowest carbonyl groups (0.99%). Therefore, the adsorption efficiency of biochars for phenol removal is not only based on the porosity of biochars but also on the oxygen containing functional groups (especially carbonyl groups).

*3.5.*Effect of Temperature and adsorption isotherm study

Temperature also affects the adsorption capacity of the adsorbents. Fig. 10 shows the plots for adsorption isotherms between q_e versus C_e at different temperatures i.e. 298K, 308K and 318K. It was observed that adsorption decreased at higher temperature; maximum adsorption followed

the order 298K > 308K > 318K. Fig.10 also depicts that at lower phenol concentrations, q_e raised sharply and thereafter the increase was gradual in the solution. Increase in temperature, from 298 K to 318 K led to decrease in adsorption, which points towards the possibility of physical adsorption and suggested weak adsorption between phenol and biochar active sites. Since adsorption is an exothermic process, it would be expected that an increase in temperature would result in decreased adsorption capacity which also corresponds to the present study. Further, it can also be understood by the increase in entropy of adsorbed molecules at surface did not recompense with increase in intermolecular interactions. As a result the increase in temperature led to decrease in adsorption performance. Similar results has also been reported by [51]. Earlier, it is also shown that the adsorption process was also being controlled by the diffusion process. Then the adsorption capacity would show an increase with an increase in temperatures due to decreased retarding forces acting on the phenolate ions which increased the mobility of ions, thereby increasing the sorptive capacity of adsorbent. But, as has been mentioned earlier, the diffusion of phenol into pores of the biochar is not the only rate-controlling step so; the diffusion process could be ignored with adequate contact time. Therefore, the decrease in sorption capacity with an increase in temperature may be attributed to physical adsorption. Further, the adsorption isotherms have been used to describe how molecules of adsorbate are adsorbed onto the adsorbent at equilibrium as a function of concentration. In this study, two isotherm models, i.e. Langmuir and Freundlich have been used. Langmuir isotherm which is based on monolayer adsorption also suggests that there is no lateral interaction between the adsorbed molecules. The non-linear form of Langmuir isotherm equation can be expressed by the following (Eq. (11)):

$$qe = (q_{max} b . C_e)/(1 + b . C_e) \quad (11)$$

Where C_e is the equilibrium concentration (mg/L) and b (L/mg) is the Langmuir adsorption constant. And, q_{max} (mg/g) is the adsorption capacity. Also, another essential characteristic of Langmuir isotherm is the equilibrium parameter R_L which is given by following equation (Eq. (12)) that defines the type of adsorption; favorable ($0 < R_L < 1$) , unfavorable ($R_L > 1$), and linear ($R_L=1$).

$$R_L = 1/(1 + b.C_0) \quad (12)$$

Apart from this, Freundlich isotherm model describes multilayer adsorption of adsorbate on active sites on adsorbent. The Freundlich isotherm is expressed as shown in equation (Eq. (13)).

$$q_e = k_f C_e^{1/n} \quad (13)$$

Where K_f is Freundlich constant of the adsorbent (mg/g (l/mg) and the values of $1/n$ are the heterogeneity factor where the value of 1/n below to 1, suggests a normal Langmuir isotherm, while 1/n > 1 indicates supportive adsorption. The non-linear fittings are shown in Fig 10. The results of this fitting are summarized in Table 5. According to this table, the phenol adsorption data were best fitted by the Langmuir model with the highest R^2 values (0.97 to 0.99). The q_{max} value obtained from Langmuir model is 41.93 mg/g, at 298 K for ACB-300. All equilibrium parameters R_L value was between 0 and 1; hence, the adsorption is considered favorable. This result shows that equilibrium adsorption capacity obtained in this study is clearly higher than some of the studies conducted with activated carbon [10][52].

*3.6.*Thermodynamic study

The effects of temperature were further investigated using thermodynamic parameters to check the spontaneity and feasibility of the adsorption process. Usually, thermodynamic parameters,

that is, heat of enthalpy (ΔH), Gibbs free energy (ΔG), and entropy (ΔS) are major parameters which govern the feasibility and spontaneity given by the following equation (Eq. (14));

$$\Delta G = -RTlnk_d \quad (14)$$

The equilibrium constant K_d has been estimated by multiplying Langmuir constant b by the molar mass of phenol (94.11 g/mol) and by 1000 then by 55.5 number of moles of pure water in one liter [53][54][55]. The thermodynamic parameters ΔG, ΔH and ΔS are summarized in Table 6.

$$\Delta G = \Delta H - T\Delta S \quad (15)$$

The value of enthalpy (ΔH) and entropy (ΔS) are calculated from the Van't Hoff equation which is obtained by plotting lnk_L and t^1/2 Fig. 11. Where the values of ΔH and ΔS were obtained from the slope and intercept, respectively

$$lnK_d = \Delta s/R - \Delta H/RT \quad (16)$$

Where R is gas constant (8.314 J/mol K) and T represent the temperature in K. The estimated values of Gibbs free energy (ΔG) were negative, which confirmed the adsorption was feasible and thermodynamically spontaneous. The negative values of ΔG increases with increase in temperature and the same results were also found in different studied using other adsorbate and adsorbents [10]. The negative values of ΔH suggested the exothermic and physisorption property of adsorption thereby demonstrating that the process was energetically stable. In addition, the value of ΔG is less than 40 KJ/mol for each biochar, which also confirmed the involved mechanism of physical adsorption. The positive values of ΔS suggested higher randomness at the solid/solution interface during the adsorption.

4. Desorption and reusability

To evaluate the possibility of regeneration and reuse the biochar, adsorption-desorption experiment were performed. Fig. 12 shows desorption study with 3 desorbing agents in which NaCl shows minimum desorption percentage whereas, NaOH shows maximum desorption percentage. From the desorption experiment performed it was concluded that with increasing number of cycles desorption percentage decreases which reveals that adsorption is not completely reversible. In other word, a part of phenol is irreversibly adsorbed on biochar which might be the results of heterogeneity of material surface or because of the multifunctional nature of adsorbent**.**

In reusability experiment (Fig. 13), shows the relationship between number of reuse cycle and % adsorption/desorption capacity of regenerated material. In biochar it is observed that both adsorption percentage desorption percentage decreases with sorption-desorption cycle. It is justified by the NaOH which is used to isolate the phenol from active sites of sorbents competes with the species of phenol which sits on the active sites. The attachment of hydroxide ions to the surface of sorbents prevents phenol from being adsorbed again in next cycles. However, with increase in number of cycles the efficiency of regeneration of biochar decreases.

5. Comparison with other prepared adsorbent

A comparison has been made between prepared biochars and previously reported plant based adsorbents for phenol removal (Table 7). As all the compared materials are of Lignocellulosic origin, the costs of these materials were considered to comparable to each other. Hence for comparison, maximum adsorption capacity was considered.

6. Conclusion

The development of biochar from Araucaria Columnaris bark was observed as cost effective and a good adsorbent for the phenol removal from aqueous solution. The iodine number (453.3 mg) obtained from experiment has acceptable range mentioned in the literature. The adsorption process was reliant on the solution pH and ionic strength. Three kinetic models were used to adjust the adsorption and the best fit was the pseudo-second order kinetic model. However, the Intraparticle diffusion model gave two linear regions which suggested that the adsorption can also be followed by multiple adsorptions. An analytical comparison shows that prepared biochar can be of useful for many other contaminants in terms of adsorption capacity. After three successive adsorption regeneration cycles, the activated biochar exhibited high phenol removal capacity (60%), good stability and high regenerability.

Acknowledgements

NA

Authors' contributions

Dinesh Chandola: Experimental work, data interpretation and Original Draft writing. Pooja Thathola: conceptualization, Review & Editing. Ankit Bisht: data validation and supervision experimental work

Funding

This work has not received any funding

Availability of data and materials

All data generated or analyzed during this study are available from the corresponding author on reasonable request.

Declarations

The authors declare they have no competing interests.

Author details

[1] center for land and water resource management, G, B Pant National Institute of Himalayan Environment, Kosi-Katarmal, Almora-263643, India

[2] IMS unison University, Dehradun-248001, India

7. Reference:

[1] H. Catherine, M. Penninckx, and D. Frédéric, “Product formation from phenolic compounds removal by laccases: A review,” *Environ. Technol. Innov.*, vol. 5, pp. 250–266, Apr. 2016, doi: 10.1016/J.ETI.2016.04.001.

[2] S. Mohammadi, A. Kargari, H. Sanaeepur, K. Abbassian, A. Najafi, and E. Mofarrah, “Phenol removal from industrial wastewaters: a short review,” *Desalin. Water Treat.*, vol. 53, no. 8, pp. 2215–2234, 2015, doi: 10.1080/19443994.2014.883327.

[3] G. Busca, S. Berardinelli, C. Resini, and L. Arrighi, “Technologies for the removal of phenol from fluid streams: A short review of recent developments,” *J. Hazard. Mater.*, vol. 160, no. 2–3, pp. 265–288, Dec. 2008, doi: 10.1016/J.JHAZMAT.2008.03.045.

[4] N. Ivanova, V. Gugleva, M. Dobreva, I. Pehlivanov, S. Stefanov, and V. Andonova, “Phenolic Compounds in Water: Sources, Reactivity, Toxicity and Treatment Methods,” *Intech*, vol. i, no. tourism, p. 13, 2016.

[5] M. J. Scott and M. N. Jones, “The biodegradation of surfactants in the environment,” *Biochim. Biophys. Acta - Biomembr.*, vol. 1508, no. 1–2, pp. 235–251, Nov. 2000, doi: 10.1016/S0304-4157(00)00013-7.

[6] B. Ba Mohammed *et al.*, “Adsorptive removal of phenol using faujasite-type Y zeolite: Adsorption isotherms, kinetics and grand canonical Monte Carlo simulation studies,” *J. Mol. Liq.*, vol. 296, p. 111997, Dec. 2019, doi: 10.1016/J.MOLLIQ.2019.111997.

[7] M. Umar and H. Abdul, “Photocatalytic degradation of organic pollutants in water,” in *Organic Pollutants - Monitoring, Risk and Treatment*, InTech, 2013, p. 15.

[8] S. Mukherjee, S. Kumar, A. K. Misra, and M. Fan, “Removal of phenols from water environment by activated carbon, bagasse ash and wood charcoal,” *Chem. Eng. J.*, vol. 129, no. 1–3, pp. 133–142, May 2007, doi: 10.1016/J.CEJ.2006.10.030.

[9] C. R. Girish and V. R. Murty, “Adsorption of phenol from wastewater using locally available adsorbents,” *J. Environ. Res. Dev.*, vol. 6, no. 3, pp. 763–772, 2012, [Online]. Available: http://www.jerad.org/ppapers/dnload.php?vl=6&is=3A&st=763.

[10] N. A. S. Mohammed, R. A. Abu-Zurayk, I. Hamadneh, and A. H. Al-Dujaili, “Phenol adsorption on biochar prepared from the pine fruit shells: Equilibrium, kinetic and thermodynamics studies,” *J. Environ. Manage.*, vol. 226, no. August, pp. 377–385, 2018, doi: 10.1016/j.jenvman.2018.08.033.

[11] S. Lv, C. Li, J. Mi, and H. Meng, “A functional activated carbon for efficient adsorption of phenol derived from pyrolysis of rice husk, KOH-activation and EDTA-4Na-modification,” *Appl. Surf. Sci.*, vol. 510, p. 145425, Apr. 2020, doi: 10.1016/J.APSUSC.2020.145425.

[12] H. M. Jang and E. Kan, “Engineered biochar from agricultural waste for removal of tetracycline in water,” *Bioresour. Technol.*, vol. 284, pp. 437–447, Jul. 2019, doi: 10.1016/J.BIORTECH.2019.03.131.

[13] K. Sun, M. Keiluweit, M. Kleber, Z. Pan, and B. Xing, “Sorption of fluorinated herbicides to plant biomass-derived biochars as a function of molecular structure,” *Bioresour. Technol.*, vol. 102, no. 21, pp. 9897–9903, 2011, doi: 10.1016/j.biortech.2011.08.036.

[14] Q. Huang, S. Song, Z. Chen, B. Hu, J. Chen, and X. Wang, “Biochar-based materials and

their applications in removal of organic contaminants from wastewater: state-of-the-art review," *Biochar*, vol. 1, pp. 45–73, 2019, doi: 10.1007/s42773-019-00006-5.

[15] M. F. Hassan, M. A. Sabri, H. Fazal, A. Hafeez, N. Shezad, and M. Hussain, "Recent trends in activated carbon fibers production from various precursors and applications—A comparative review," *J. Anal. Appl. Pyrolysis*, vol. 145, p. 104715, Jan. 2020, doi: 10.1016/J.JAAP.2019.104715.

[16] O. G. Sas, P. B. Sánchez, B. González, and Á. Domínguez, "Removal of phenolic pollutants from wastewater streams using ionic liquids," *Sep. Purif. Technol.*, vol. 236, p. 116310, Apr. 2020, doi: 10.1016/J.SEPPUR.2019.116310.

[17] J. G. S. Medeiros, M. Tomazello Fo., F. J. Krug, and A. E. S. Vives, "Tree-ring characterization of Araucaria columnaris Hook and its applicability as a lead indicator in environmental monitoring," *Dendrochronologia*, vol. 26, no. 3, pp. 165–171, Dec. 2008, doi: 10.1016/J.DENDRO.2008.07.002.

[18] A. Demirbas, "Effects of temperature and particle size on bio-char yield from pyrolysis of agricultural residues," vol. 72, pp. 243–248, 2004, doi: 10.1016/j.jaap.2004.07.003.

[19] S. L. Goertzen, K. D. Thériault, A. M. Oickle, A. C. Tarasuk, and H. A. Andreas, "Standardization of the Boehm titration. Part I. CO2 expulsion and endpoint determination," *Carbon N. Y.*, vol. 48, no. 4, pp. 1252–1261, 2010, doi: 10.1016/j.carbon.2009.11.050.

[20] L. D. Hafshejani *et al.*, "Removal of zinc and lead from aqueous solution by nanostructured cedar leaf ash as biosorbent," *J. Mol. Liq.*, vol. 211, pp. 448–456, 2015,

doi: 10.1016/j.molliq.2015.07.044.

[21] D. Özçimen and A. Ersoy-Meriçboyu, "A study on the carbonization of grapeseed and chestnut shell," *Fuel Process. Technol.*, vol. 89, no. 11, pp. 1041–1046, 2008, doi: 10.1016/j.fuproc.2008.04.006.

[22] H. S. Kambo and A. Dutta, "A comparative review of biochar and hydrochar in terms of production, physico-chemical properties and applications," *Renew. Sustain. Energy Rev.*, vol. 45, pp. 359–378, May 2015, doi: 10.1016/J.RSER.2015.01.050.

[23] F. Ronsse, S. van Hecke, D. Dickinson, and W. Prins, "Production and characterization of slow pyrolysis biochar: Influence of feedstock type and pyrolysis conditions," *GCB Bioenergy*, vol. 5, no. 2, pp. 104–115, 2013, doi: 10.1111/gcbb.12018.

[24] J. Zhang, J. Liu, and R. Liu, "Effects of pyrolysis temperature and heating time on biochar obtained from the pyrolysis of straw and lignosulfonate," *Bioresour. Technol.*, vol. 176, pp. 288–291, 2015, doi: 10.1016/j.biortech.2014.11.011.

[25] R. Zornoza, F. Moreno-Barriga, J. A. Acosta, M. A. Muñoz, and A. Faz, "Stability, nutrient availability and hydrophobicity of biochars derived from manure, crop residues, and municipal solid waste for their use as soil amendments," *Chemosphere*, vol. 144, pp. 122–130, 2016, doi: 10.1016/j.chemosphere.2015.08.046.

[26] E. Taskin, C. de Castro Bueno, I. Allegretta, R. Terzano, A. H. Rosa, and E. Loffredo, "Multianalytical characterization of biochar and hydrochar produced from waste biomasses for environmental and agricultural applications," *Chemosphere*, vol. 233, pp. 422–430, Oct. 2019, doi: 10.1016/J.CHEMOSPHERE.2019.05.204.

[27] A. R. A. Usman *et al.*, "Biochar production from date palm waste: Charring temperature induced changes in composition and surface chemistry," *J. Anal. Appl. Pyrolysis*, vol. 115, pp. 392–400, 2015, doi: 10.1016/j.jaap.2015.08.016.

[28] J. Cheng *et al.*, "Sulfur removal at high temperature during coal combustion in furnaces: A review," *Prog. Energy Combust. Sci.*, vol. 29, no. 5, pp. 381–405, 2003, doi: 10.1016/S0360-1285(03)00030-3.

[29] W. Suliman, J. B. Harsh, N. I. Abu-Lail, A. M. Fortuna, I. Dallmeyer, and M. Garcia-Perez, "Influence of feedstock source and pyrolysis temperature on biochar bulk and surface properties," *Biomass and Bioenergy*, vol. 84, pp. 37–48, 2016, doi: 10.1016/j.biombioe.2015.11.010.

[30] W. Wang, M. Li, and Q. Zeng, "Adsorption of chromium (VI) by strong alkaline anion exchange fiber in a fixed-bed column: Experiments and models fitting and evaluating," *Sep. Purif. Technol.*, vol. 149, no. 5, pp. 16–23, 2015, doi: 10.1016/j.seppur.2015.05.022.

[31] M. A. Mohammad Razi, A. Al-Gheethi, M. Al-Qaini, and A. Yousef, "Efficiency of activated carbon from palm kernel shell for treatment of greywater," *Arab J. Basic Appl. Sci.*, vol. 25, no. 3, pp. 103–110, 2018, doi: 10.1080/25765299.2018.1514142.

[32] A. Mukherjee, A. R. Zimmerman, and W. Harris, "Surface chemistry variations among a series of laboratory-produced biochars," *Geoderma*, vol. 163, no. 3–4, pp. 247–255, 2011, doi: 10.1016/j.geoderma.2011.04.021.

[33] S. A. Doydora, M. L. Cabrera, K. C. Das, J. W. Gaskin, L. S. Sonon, and W. P. Miller, "Release of nitrogen and phosphorus from poultry litter amended with acidified biochar,"

Int. J. Environ. Res. Public Health, vol. 8, no. 5, pp. 1491–1502, 2011, doi: 10.3390/ijerph8051491.

[34] L. Sun, S. Wan, and W. Luo, "Biochars prepared from anaerobic digestion residue, palm bark, and eucalyptus for adsorption of cationic methylene blue dye: Characterization, equilibrium, and kinetic studies," *Bioresour. Technol.*, vol. 140, pp. 406–413, 2013, doi: 10.1016/j.biortech.2013.04.116.

[35] L. Lonappan, Y. Liu, T. Rouissi, S. K. Brar, and R. Y. Surampalli, "Development of biochar-based green functional materials using organic acids for environmental applications," *J. Clean. Prod.*, vol. 244, p. 118841, Jan. 2020, doi: 10.1016/J.JCLEPRO.2019.118841.

[36] D. Mohan, A. Sarswat, V. K. Singh, M. Alexandre-Franco, and C. U. Pittman, "Development of magnetic activated carbon from almond shells for trinitrophenol removal from water," *Chem. Eng. J.*, vol. 172, no. 2–3, pp. 1111–1125, Aug. 2011, doi: 10.1016/J.CEJ.2011.06.054.

[37] R. Powar and T. Talsande, "Effect of temperature on iodine value and total carbon contain in," no. February 2015, 2018, doi: 10.15740/HAS/IJAE/8.1/26-30.

[38] J. H. Tay, X. G. Chen, S. Jeyaseelan, and N. Graham, "Optimising the preparation of activated carbon from digested sewage sludge and coconut husk," *Chemosphere*, vol. 44, no. 1, pp. 45–51, 2001, doi: 10.1016/S0045-6535(00)00383-0.

[39] B. H. Hameed and A. A. Rahman, "Removal of phenol from aqueous solutions by adsorption onto activated carbon prepared from biomass material," *J. Hazard. Mater.*, vol.

160, no. 2–3, pp. 576–581, 2008, doi: 10.1016/j.jhazmat.2008.03.028.

[40] C. Moreno-Castilla, “Adsorption of organic molecules from aqueous solutions on carbon materials,” *Carbon N. Y.*, vol. 42, no. 1, pp. 83–94, 2004, doi: 10.1016/j.carbon.2003.09.022.

[41] T. Islam *et al.*, “Journal of Environmental Chemical Engineering Removal of methylene blue and tetracycline from water using peanut shell derived adsorbent prepared by sulfuric acid re fl ux,” *J. Environ. Chem. Eng.*, vol. 7, no. 1, p. 102816, 2019, doi: 10.1016/j.jece.2018.102816.

[42] Q. Shen *et al.*, “Removal of tetracycline from an aqueous solution using manganese dioxide modified biochar derived from Chinese herbal medicine residues,” *Environ. Res.*, vol. 183, p. 109195, Apr. 2020, doi: 10.1016/J.ENVRES.2020.109195.

[43] C. Jeon, K. L. Solis, H.-R. An, Y. Hong, A. D. Igalavithana, and Y. S. Ok, “Sustainable removal of Hg(II) by sulfur-modified pine-needle biochar,” *J. Hazard. Mater.*, vol. 388, p. 122048, Apr. 2020, doi: 10.1016/J.JHAZMAT.2020.122048.

[44] V. Fierro, V. Torné-Fernández, D. Montané, and A. Celzard, “Adsorption of phenol onto activated carbons having different textural and surface properties,” *Microporous Mesoporous Mater.*, vol. 111, no. 1–3, pp. 276–284, 2008, doi: 10.1016/j.micromeso.2007.08.002.

[45] L. A. Rodrigues, M. L. C. P. da Silva, M. O. Alvarez-Mendes, A. dos R. Coutinho, and G. P. Thim, “Phenol removal from aqueous solution by activated carbon produced from avocado kernel seeds,” *Chem. Eng. J.*, vol. 174, no. 1, pp. 49–57, 2011, doi:

10.1016/j.cej.2011.08.027.

[46] R. W. Coughlin and F. S. Ezra, “Role of Surface Acidity in the Adsorption of Organic Pollutants on the Surface of Carbon,” *Environ. Sci. Technol.*, vol. 2, no. 4, pp. 291–297, 1968, doi: 10.1021/es60016a002.

[47] J. M. V. Nabais, J. A. Gomes, Suhas, P. J. M. Carrott, C. Laginhas, and S. Roman, “Phenol removal onto novel activated carbons made from lignocellulosic precursors: Influence of surface properties,” *J. Hazard. Mater.*, vol. 167, no. 1–3, pp. 904–910, 2009, doi: 10.1016/j.jhazmat.2009.01.075.

[48] J. A. Mattson, H. B. Mark, M. D. Malbin, W. J. Weber, and J. C. Crittenden, “Surface chemistry of active carbon: Specific adsorption of phenols,” *J. Colloid Interface Sci.*, vol. 31, no. 1, pp. 116–130, 1969, doi: 10.1016/0021-9797(69)90089-7.

[49] A. P. Terzyk, “Further insights into the role of carbon surface functionalities in the mechanism of phenol adsorption,” *J. Colloid Interface Sci.*, vol. 268, no. 2, pp. 301–329, 2003, doi: 10.1016/S0021-9797(03)00690-8.

[50] D. Zhang, P. Huo, and W. Liu, “Behavior of phenol adsorption on thermal modified activated carbon,” *Chinese J. Chem. Eng.*, vol. 24, no. 4, pp. 446–452, 2016, doi: 10.1016/j.cjche.2015.11.022.

[51] O. Abdelwahab and N. K. Amin, “Adsorption of phenol from aqueous solutions by Luffa cylindrica fibers: Kinetics, isotherm and thermodynamic studies,” *Egypt. J. Aquat. Res.*, vol. 39, no. 4, pp. 215–223, 2013, doi: 10.1016/j.ejar.2013.12.011.

[52] V. C. Srivastava, M. M. Swamy, I. D. Mall, B. Prasad, and I. M. Mishra, “Adsorptive

removal of phenol by bagasse fly ash and activated carbon: Equilibrium, kinetics and thermodynamics," *Colloids Surfaces A Physicochem. Eng. Asp.*, vol. 272, no. 1–2, pp. 89–104, 2006, doi: 10.1016/j.colsurfa.2005.07.016.

[53] H. N. Tran, S. J. You, A. Hosseini-Bandegharaei, and H. P. Chao, "Mistakes and inconsistencies regarding adsorption of contaminants from aqueous solutions: A critical review," *Water Res.*, vol. 120, pp. 88–116, 2017, doi: 10.1016/j.watres.2017.04.014.

[54] H. N. Tran, S. J. You, and H. P. Chao, "Fast and efficient adsorption of methylene green 5 on activated carbon prepared from new chemical activation method," *J. Environ. Manage.*, vol. 188, no. 2017, pp. 322–336, 2017, doi: 10.1016/j.jenvman.2016.12.003.

[55] H. N. Tran, S. J. You, T. V. Nguyen, and H. P. Chao, "Insight into the adsorption mechanism of cationic dye onto biosorbents derived from agricultural wastes," *Chem. Eng. Commun.*, vol. 204, no. 9, pp. 1020–1036, 2017, doi: 10.1080/00986445.2017.1336090.

[56] B. H. Hameed, L. H. Chin, and S. Rengaraj, "Adsorption of 4-chlorophenol onto activated carbon prepared from rattan sawdust," *Desalination*, vol. 225, no. 1–3, pp. 185–198, May 2008, doi: 10.1016/J.DESAL.2007.04.095.

[57] M. Z. Alam, E. S. Ameem, S. A. Muyibi, and N. A. Kabbashi, "The factors affecting the performance of activated carbon prepared from oil palm empty fruit bunches for adsorption of phenol," *Chem. Eng. J.*, vol. 155, no. 1–2, pp. 191–198, Dec. 2009, doi: 10.1016/J.CEJ.2009.07.033.

[58] M. Sathishkumar, A. R. Binupriya, D. Kavitha, and S. E. Yun, "Kinetic and isothermal

studies on liquid-phase adsorption of 2,4-dichlorophenol by palm pith carbon," *Bioresour. Technol.*, vol. 98, no. 4, pp. 866–873, Mar. 2007, doi: 10.1016/J.BIORTECH.2006.03.002.

[59] Z. Hao, C. Wang, Z. Yan, H. Jiang, and H. Xu, "Magnetic particles modification of coconut shell-derived activated carbon and biochar for effective removal of phenol from water," *Chemosphere*, vol. 211, pp. 962–969, Nov. 2018, doi: 10.1016/J.CHEMOSPHERE.2018.08.038.

List of figures

List of tables

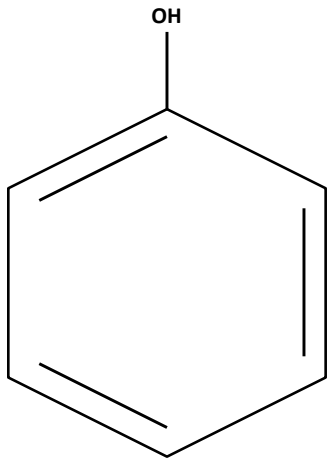

Fig. 1 physical structure of phenol

Fig. 2 bark of araucaria Columnaris tree

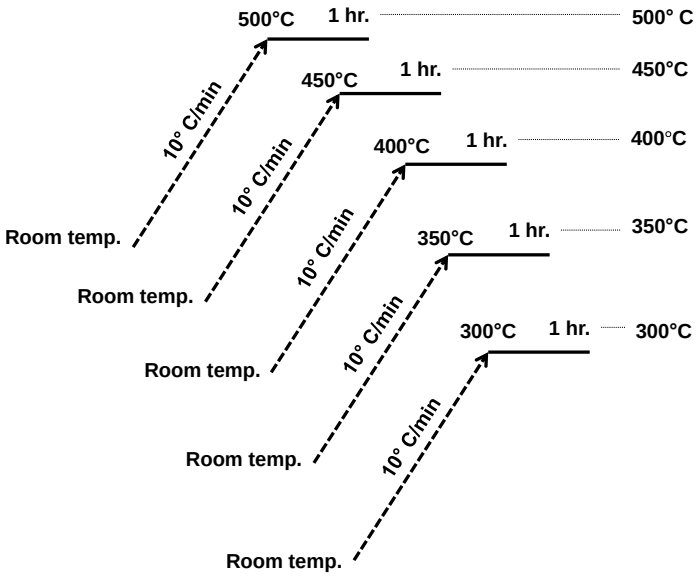

Fig. 3 Temperature program for pyrolysis process

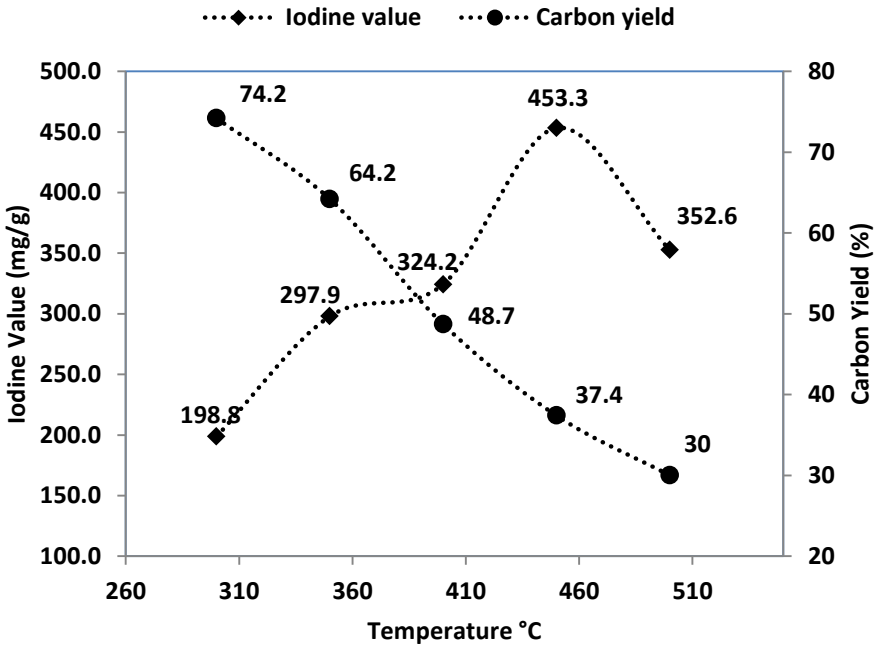

Fig. 4 Biochar yield vs. Iodine Value

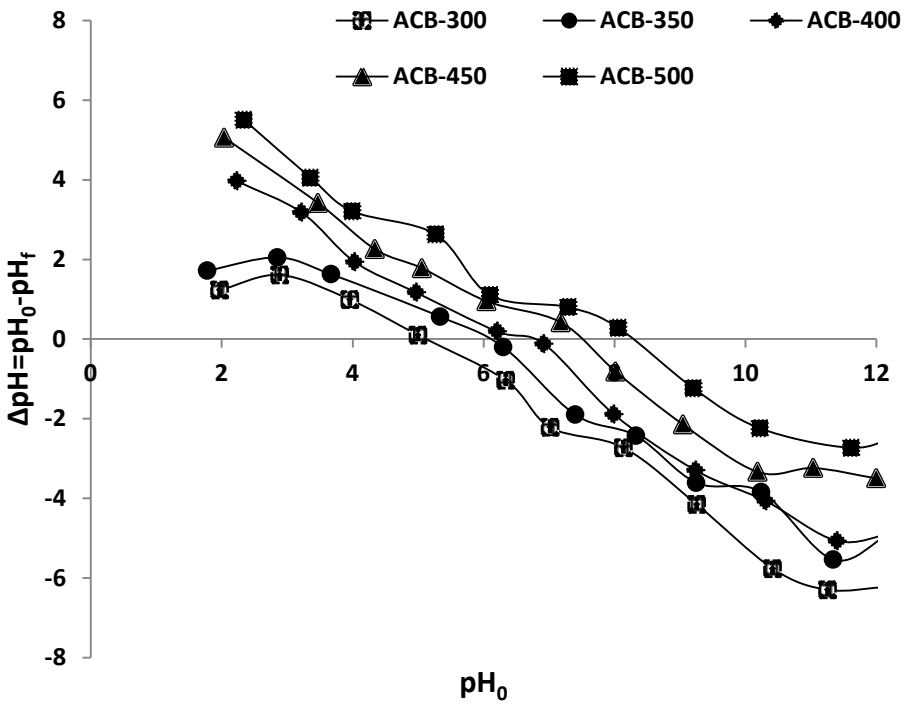

Fig. 5 pH_{pzc} of biochar

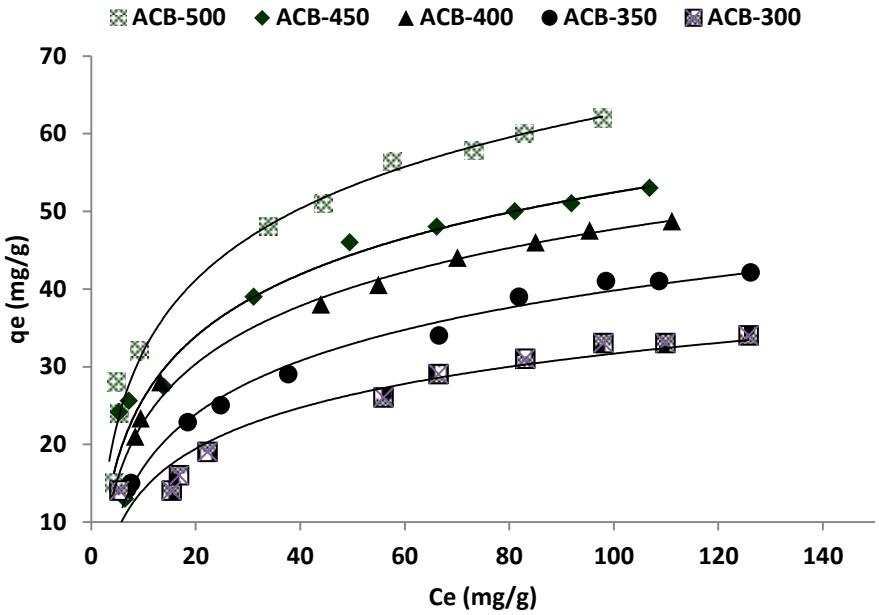

Fig. 6 Effect of Initial Concentration

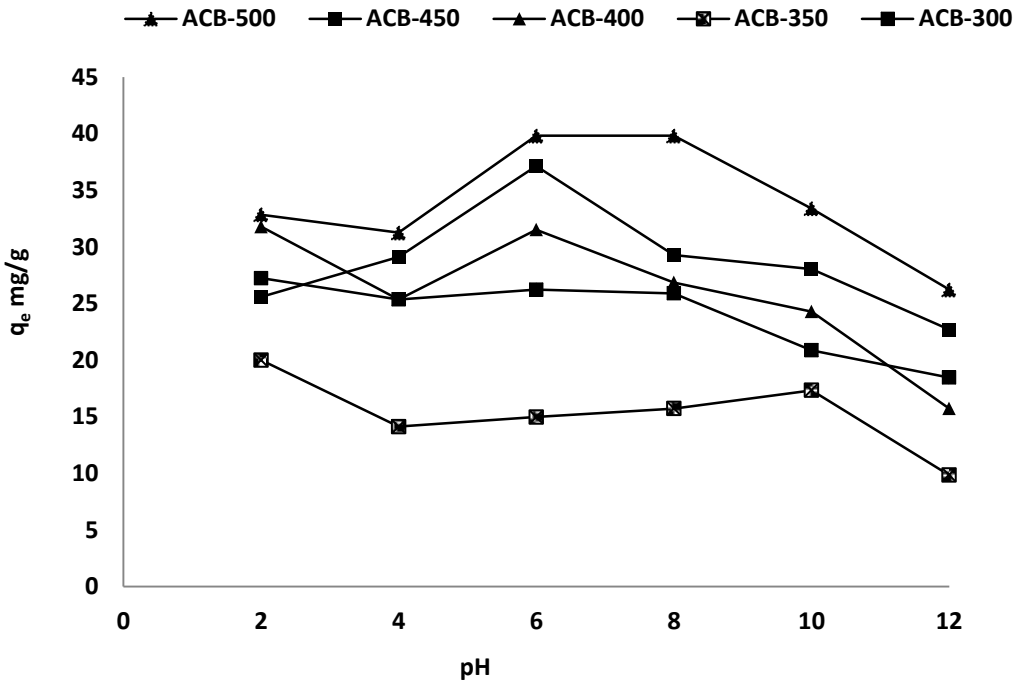

Fig. 7 Effect of pH on phenol adsorption

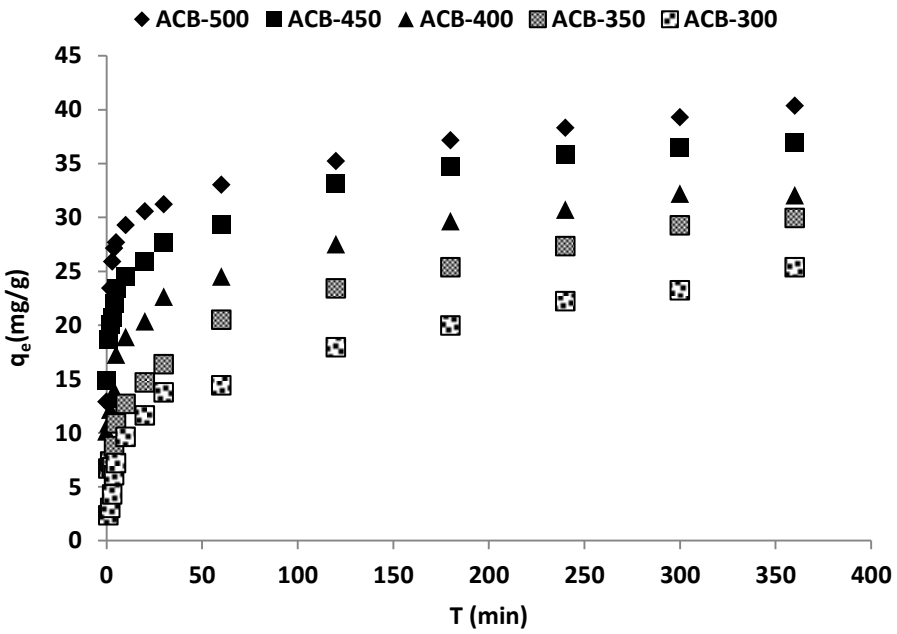

Fig. 8 Effect of Contact time on phenol removal

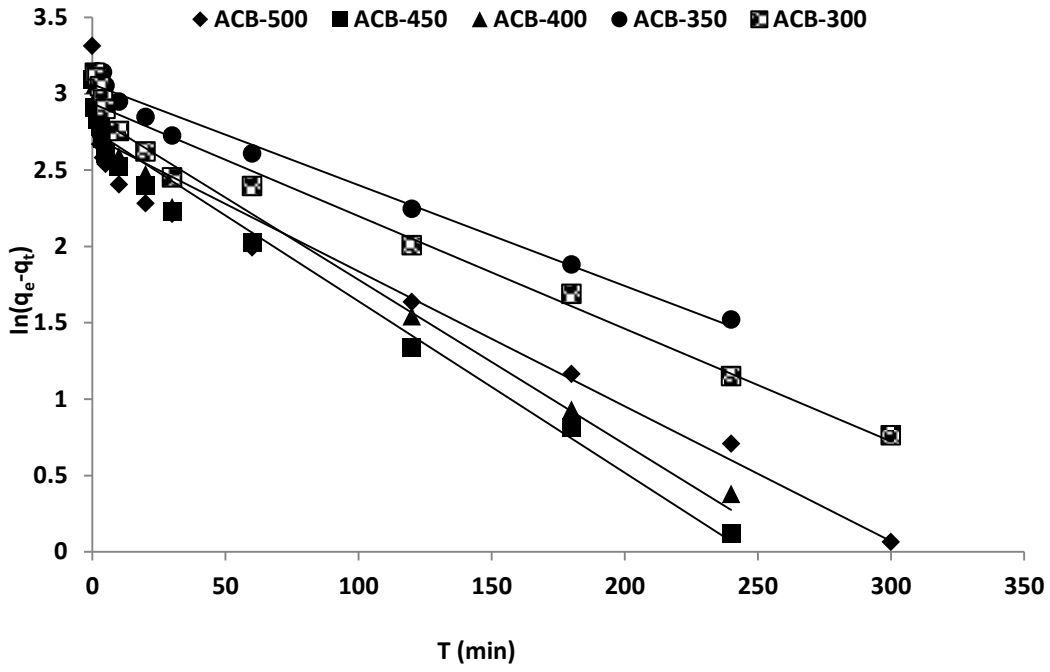

Fig. 9A Pseudo first order reaction kinetics

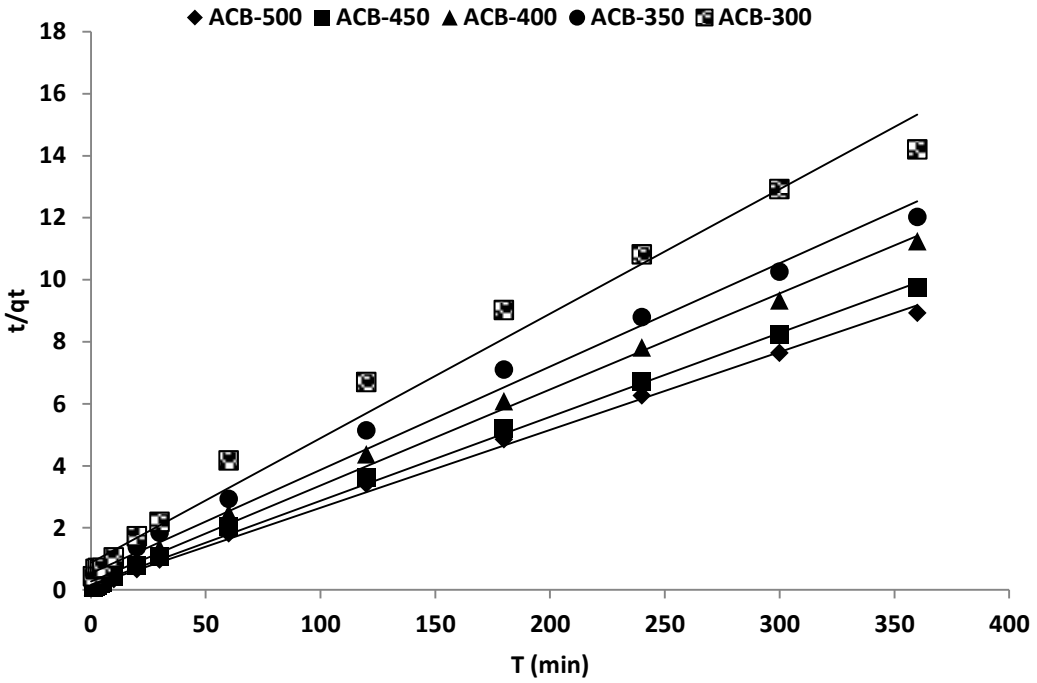

Fig. 9B Pseudo second order reaction kinetics

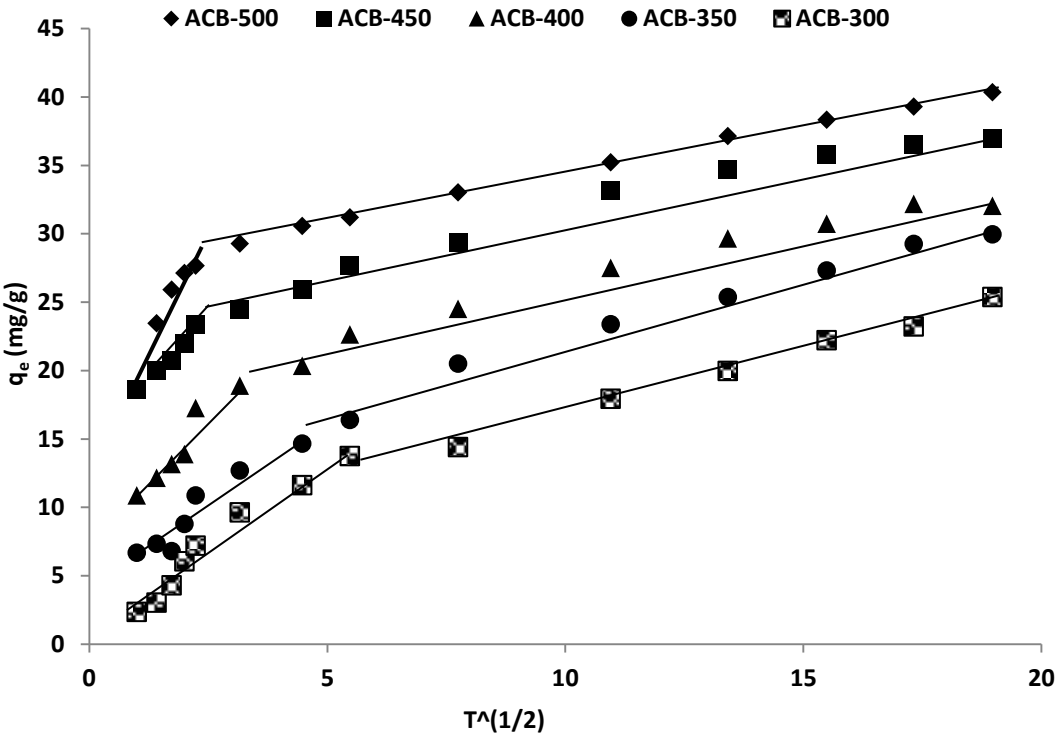

Fig. 9C Intra-particle reaction kinetics

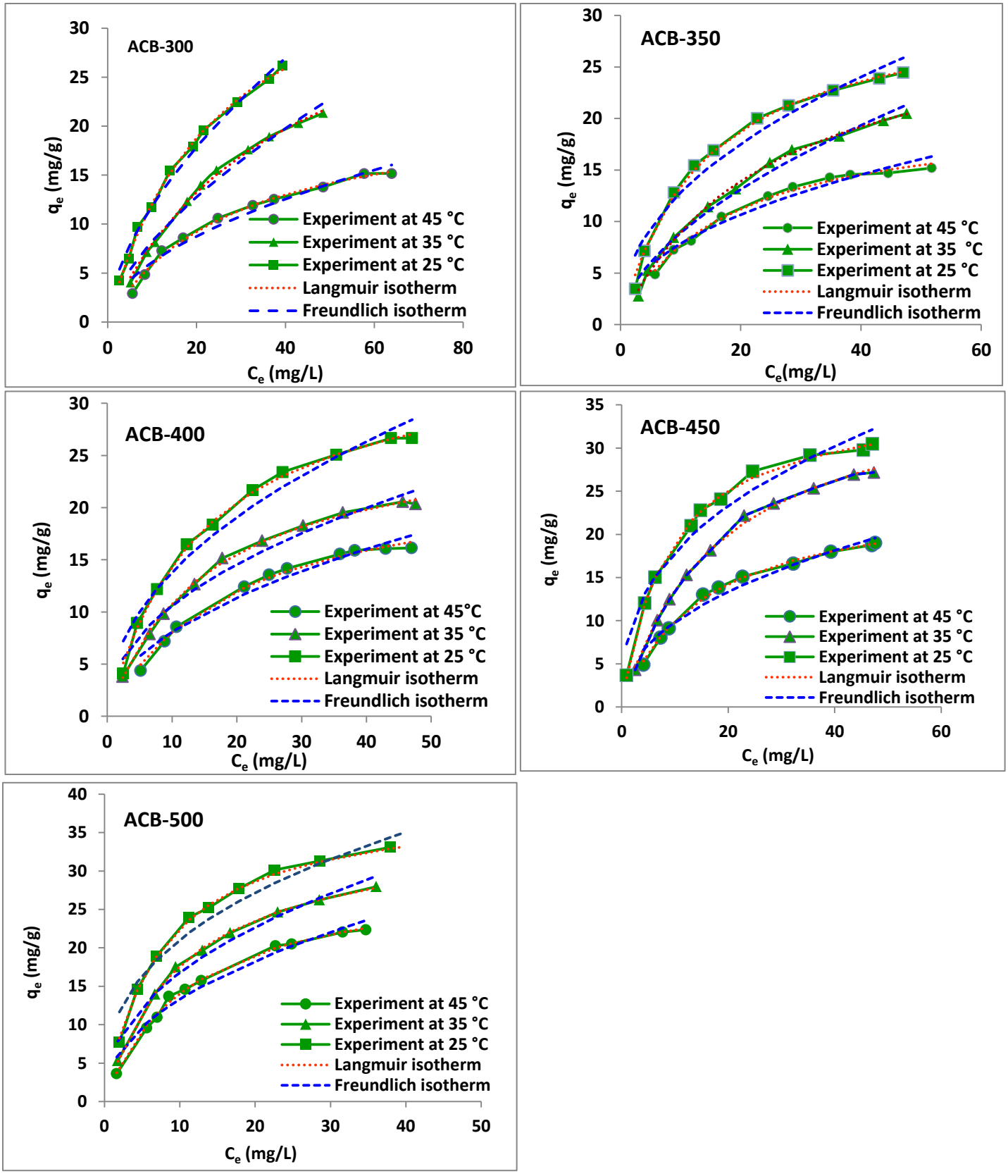

Fig. 10 Effect of temp and isotherm model

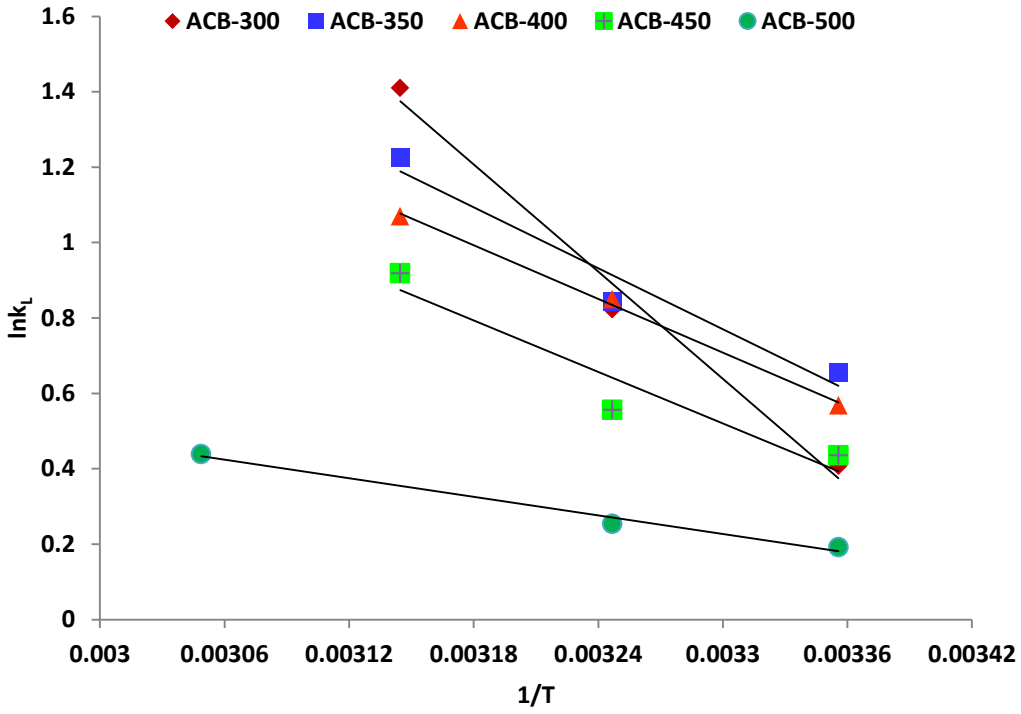

Fig. 11 Van't Hoff Plot

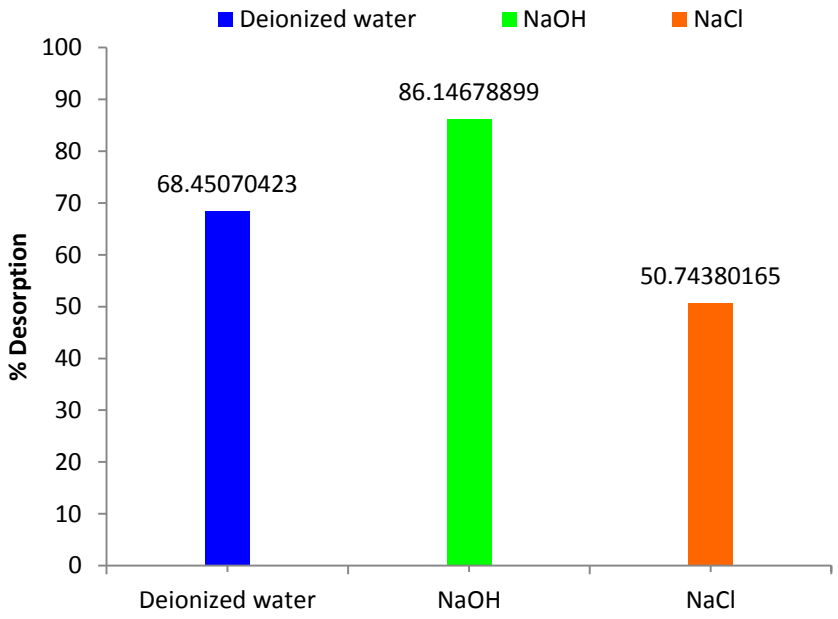

Fig. 12 Desorption study

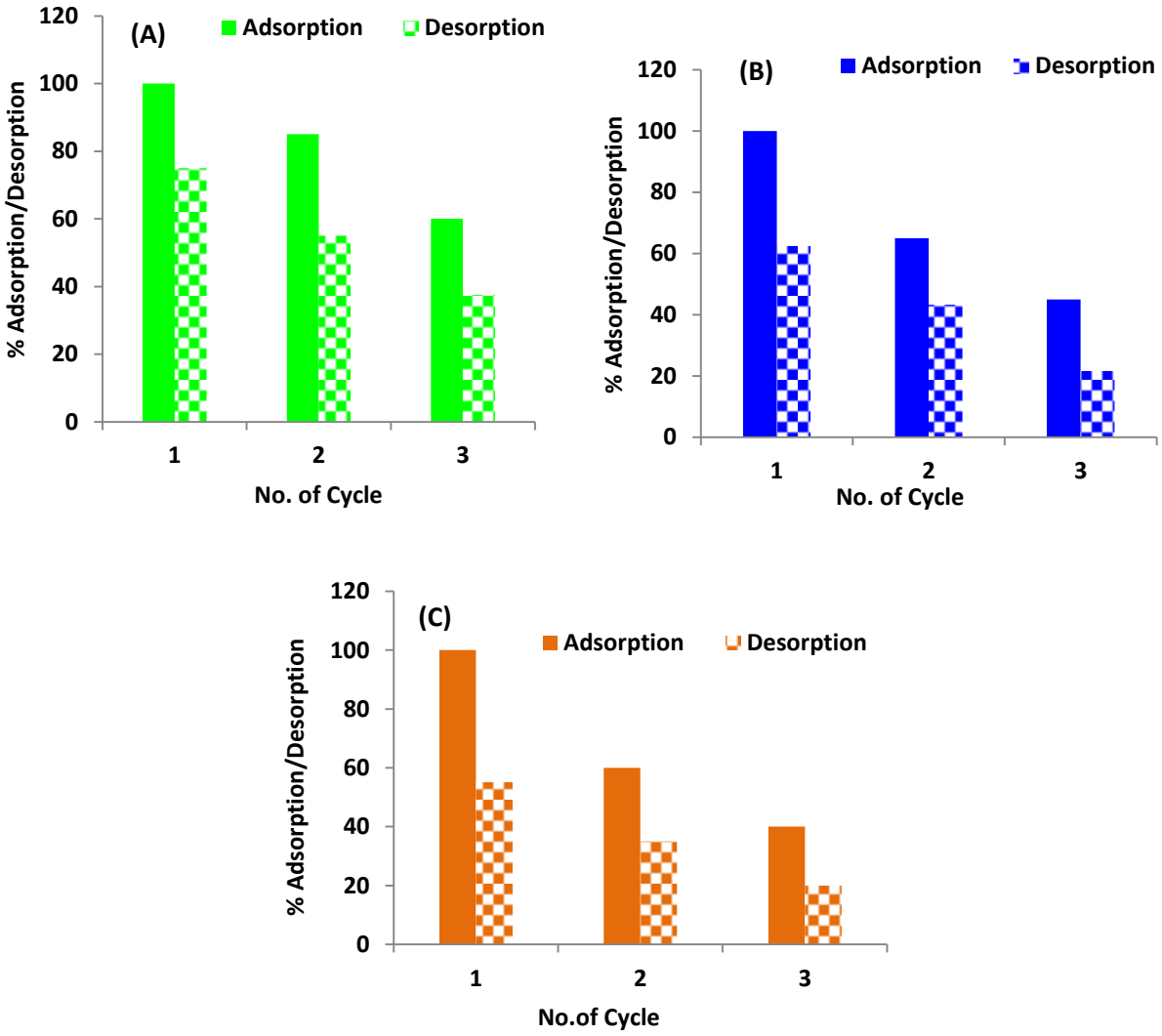

Fig. 13 Desorption/Adsorption (a); Desorption by NaOH (b); Desorption by Deionized water (C); Desorption by NaCl

Table 1. Tested properties of the biochar using different pyrolysis temperature

Process conditions		Proximate analysis					
Pyrolysis temp (°C)	**Residence time (min)**	**Biochar yield (Wt. %)**	**Volatile matter (Wt. %)**	**Fixed carbon (Wt. %)**	**Ash content (Wt. %)**	**Fixed carbon yield (Wt. %)**	**pH in solution**
ACB-300	**60**	74.2	49.4	22.54	3.4	17.8	4.7
ACB-350	**60**	64.4	62.3	34.58	5.5	22.64	4.9
ACB-400	**60**	48.7	41.27	46.96	8.84	19.4	5.54
ACB-450	**60**	37.4	14.85	57.12	12.05	23.6	6.48
ACB-500	**60**	30.0	8.14	68.44	13.55	21.74	8.47

Table 2 elemental composition of Araucaria Columnaris bark biochar

Biochar	Sample Wt. (mg)	C (%)	H (%)	N (%)	S (%)	Iodine value (mg/g)
ACB-300	12.86	43.11	7.517	1.727	15.09	198.8
ACB-350	12.04	49.3	6.78	1.801	10.04	297.9
ACB-400	11.89	56.7	5.98	1.57	8.015	324.2
ACB-450	12.42	64.97	4.66	1.95	6.014	453.3
ACB-500	12.33	79.7	2.22	1.41	2.005	352.6

Table 3 Amount of various Oxygen-containing Functional Groups of biochar (mmol g-1)

	Lactone groups	Carbonyl group	Carboxylic group	Total acidic groups	Total basic groups
ACB-300	0.05	3.41	1.65	4.65	0.12
ACB-350	0.09	2.48	0.95	1.89	0.31
ACB-400	0.10	1.64	0.48	0.82	0.94
ACB-450	0.13	1.41	0.41	0.31	1.51
ACB-500	1.01	0.99	0.38	0.05	1.87

Table 4 Reaction kinetics values for three models

Biochar	Pseudo first order			Pseudo second order			Intra-particle diffusion	
	q_e (mg/g)	K_1 (/min)	R^2	q_e (mg/g)	K_1 (mg/g/min)	R^2	k_p (mg/g/min)	R^2
ACB-300	18.86	$-2.05X10^{-5}$	0.96	1.13	0.88	0.94	0.21	0.94
ACB-350	21.39	$-1.8X10^{-5}$	0.98	1.86	0.53	0.99	0.38	0.95
ACB-400	17.46	$-2.4X10^{-5}$	0.96	3.64	0.27	0.99	0.69	0.91
ACB-450	15.88	$-3.1X10^{-5}$	0.97	5.93	0.16	0.99	1.07	0.94
ACB-500	15.19	$-2.4X10^{-5}$	0.93	7.29	0.13	0.99	1.27	0.86

Table 5 Langmuir and Freundlich isotherm parameters

		Langmuir parameters			Freundlich parameters		
Biochar	**Tem (K)**	**q_{max} (mg/g)**	**b (L/mg)**	**R^2**	**k_f**	**1/n**	**R^2**
ACB-300	**298**	41.93	0.04	0.99	3.00	0.59	0.98
	308	38.74	0.02	0.97	1.91	0.63	0.97
	318	22.01	0.03	0.99	1.83	0.52	0.94
ACB-350	**298**	31.65	0.07	0.98	4.46	0.45	0.92
	308	30.96	0.04	0.98	2.80	0.44	0.95
	318	20.73	0.05	0.99	2.80	0.44	0.95
ACB-400	**298**	35.40	0.06	0.99	4.77	0.46	0.94
	308	27.42	0.06	0.99	3.70	0.45	0.96
	318	23.57	0.05	0.98	2.5	0.49	0.96
ACB-450	**298**	36.09	0.11	0.99	7.56	0.37	0.94
	308	38.27	0.05	0.99	1.00	1.00	0.96
	318	24.88	0.06	0.99	3.5	0.44	0.95
ACB-500	**298**	39.42	0.132	0.98	9.06	0.36	0.94
	308	35.73	0.09	0.99	6.13	0.43	0.96
	318	29.96	0.08	0.99	4.64	0.45	0.95

Table 6 thermodynamic parameters

Biochar sample	Temp. (K)	k_L	ΔG ($kJmol^{-1}$)	ΔH ($kJmol^{-1}$)	ΔS ($Jmol^{-1}$)
ACB-300	298	1.50	-1.01	-39.37	135.25
	308	2.27	-2.10		
	318	4.09	-3.72		
ACB-350	298	1.92	-1.62	-22.37	80.25
	308	2.32	-2.15		
	318	3.40	-3.23		
ACB-400	298	1.76	-1.40	-19.75	71.08
	308	2.33	-2.17		
	318	2.91	-2.82		
ACB-450	298	1.54	-1.07	-18.93	66.80
	308	1.74	-1.42		
	318	2.50	-2.42		
ACB-500	298	1.21	-0.47	-6.826	24.41
	308	1.28	-0.65		
	318	1.55	-1.19		

Table 7 Comparison of adsorption capacity of some of the recent plant based low-cost adsorbents for phenols removal.

S. No.	Adsorbent	Adsorption Capacity ($mg.g^{-1}$)	Ref
1	Rattan sawdust (RSAC)	188.68	[56]
2	Oil palm empty fruit bunches	0.997	[57]
3	Coconut husk	191.73	[9]
4	(a)Wood charcoal	53.2	[8]
	(b) Bagasse ash	53	[8]
5	Palm pith carbon	19.6	[58]
6	Coconut-shell AC	72.7	[59]
7	Rice carbon	14.2	[11]
8	Araucaria Columnaris, bark biochar	41.93	Present study